This article was downloaded by: [Renmin University of China]
On: 13 October 2013, At: 10:43
Publisher: Taylor & Francis
Informa Ltd Registered in England and Wales Registered Number: 1072954 Registered office: Mortimer House, 37-41 Mortimer Street, London W1T 3JH, UK

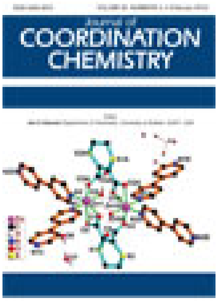

Journal of Coordination Chemistry
Publication details, including instructions for authors and subscription information:
http://www.tandfonline.com/loi/gcoo20

Crystal structures and spectroscopic analyses of two Co(II) N^6-benzylaminopurine supramolecules

Min Xia [a], Tian-Tian Chen [a], Bu-Shun Shan [a] & Chun-Li Wei [b]
[a] Jiangsu Key Laboratory for Chemistry of Low-dimensional Materials, School of Chemistry and Chemical Engineering, Huaiyin Normal University, Huaian 223300, P.R. China
[b] Department of Criminal Science and Technology, Jilin Police College, Changchun 130117, P.R. China

Published online: 31 Jan 2012.

To cite this article: Min Xia, Tian-Tian Chen, Bu-Shun Shan & Chun-Li Wei (2012) Crystal structures and spectroscopic analyses of two Co(II) N^6-benzylaminopurine supramolecules, Journal of Coordination Chemistry, 65:3, 380-392, DOI: 10.1080/00958972.2011.653351

To link to this article: http://dx.doi.org/10.1080/00958972.2011.653351

PLEASE SCROLL DOWN FOR ARTICLE

Taylor & Francis makes every effort to ensure the accuracy of all the information (the "Content") contained in the publications on our platform. However, Taylor & Francis, our agents, and our licensors make no representations or warranties whatsoever as to the accuracy, completeness, or suitability for any purpose of the Content. Any opinions and views expressed in this publication are the opinions and views of the authors, and are not the views of or endorsed by Taylor & Francis. The accuracy of the Content should not be relied upon and should be independently verified with primary sources of information. Taylor and Francis shall not be liable for any losses, actions, claims, proceedings, demands, costs, expenses, damages, and other liabilities whatsoever or howsoever caused arising directly or indirectly in connection with, in relation to or arising out of the use of the Content.

This article may be used for research, teaching, and private study purposes. Any substantial or systematic reproduction, redistribution, reselling, loan, sub-licensing, systematic supply, or distribution in any form to anyone is expressly forbidden. Terms &

Journal of Coordination Chemistry
Vol. 65, No. 3, 10 February 2012, 380–392

Crystal structures and spectroscopic analyses of two Co(II) N^6-benzylaminopurine supramolecules

MIN XIA*†, TIAN-TIAN CHEN†, BU-SHUN SHAN† and CHUN-LI WEI‡

†Jiangsu Key Laboratory for Chemistry of Low-dimensional Materials, School of Chemistry and Chemical Engineering, Huaiyin Normal University, Huaian 223300, P.R. China
‡Department of Criminal Science and Technology, Jilin Police College, Changchun 130117, P.R. China

(*Received 26 July 2011; in final form 11 November 2011*)

Two mononuclear Co(II) N^6-benzylaminopurine compounds, $[Co(6\text{-}BA\text{-}H_2)_2(H_2O)_4] \cdot (R)_2 \cdot 4.5H_2O$ (**1**) and $[Co(6\text{-}BA\text{-}H)_2(H_2O)Cl_3]Cl \cdot H_2O$ (**2**) (6-BA = N^6-benzylaminopurine $(C_5H_2N_3NH)(NH)CH_2(C_6H_5)$, H_3R = 5-sulfosalicylic acid $(C_6H_3)CO_2H(OH)SO_3H)$, are reported. Compound **1** possesses a 3-D supramolecular structure built *via* H-bond and π–π stacking interactions that contains a mononuclear six-coordinate $[Co(6\text{-}BA\text{-}H_2)_2(H_2O)_4]^{6+}$. Compound **2** also exhibits a 3-D supramolecular framework with mononuclear six-coordinate cation $[Co(6\text{-}BA\text{-}H)_2(H_2O)Cl_3]^+$. Luminescence studies at room temperature show that **1** ($\lambda_{ex} = 268$ nm) displays two strong fluorescent emissions centered at 326.8 nm and 356.9 nm, while **2** ($\lambda_{ex} = 233$ nm) exhibits a weaker peak emitted at 342.8 nm upon 6-BA-complexation of two different second ligands H_3R/Cl^- with Co(II).

Keywords: Co(II) N^6-benzylaminopurine compound; Crystal structure; Supramolecule; Fluorescence

1. Introduction

Self-assembly of supramolecular architectures of organic ligands with metal ions is currently of interest due to fascinating properties, versatile intriguing structures, and topologies, along with promising applications in the areas of catalysis, chirality, conductivity, luminescence, magnetism, and porosity [1]. Supramolecular interactions, such as hydrogen bonds, π–π stacking, and electrostatic attraction play a crucial role in properties and potential applications of inorganic–organic hybrid compounds [2]. 6-Benzylaminopurine (6-BA) is an adenine derivative with 6-substituted group, while also an *N*-heterocyclic amine. *N*-heterocyclic amines present interesting electronic, photonic, and magnetic properties when coordinated to transition metals; it is a prominent building block in organic–inorganic supramolecular chemistry because of π-stacking ability, directional H-bonding, and coordination properties. 6-Benzyl-amino substituent has high activity, which plays an important role in tissue culture, gene expression regulation, stress resistance, anti-aging, plant growth stimulants, anti-heavy

---

*Corresponding author. Email: xiamin1964@163.com

Journal of Coordination Chemistry
ISSN 0095-8972 print/ISSN 1029-0389 online © 2012 Taylor & Francis
http://dx.doi.org/10.1080/00958972.2011.653351

metal pollution, etc. [3–7]. Metal ions in life processes can lead to body lesions, so research of adenine derivatives coordinating with metal ions has significance in life sciences and material chemistry. We seek to introduce 6-BA into a synthesis system. Self-assembly to combine 6-BA with metal ion has not been well-developed. Major efforts have been devoted to the exploration of 6-BA derivatives to obtain more information about designing and building specific supramolecular architectures [8–10]. There are few reports on 6-BA compounds with metal ions [11–13]. Here, we introduce two Co(II)-6-BA compounds, $[Co(6\text{-}BA\text{-}H_2)_2(H_2O)_4]\cdot(R)_2\cdot 4.5H_2O$ (**1**) and $[Co(6\text{-}BA\text{-}H)_2(H_2O)Cl_3]Cl\cdot H_2O$ (**2**), with the solid fluorescence spectra also discussed.

2. Experimental

2.1. *Materials and physical measurements*

All chemicals purchased were of reagent grade and used without purification. Infrared (IR) spectra were recorded on an AVATAR360 spectrophotometer from 4000 to 400 cm^{-1} using KBr pellets. Elemental analyses were performed using an Optima-2000DV elemental analyzer. Absorption spectra were performed on an Australia GBC UV/Vis 916 spectrophotometer from 200 to 600 nm. Emission and excitation spectra were measured on a Perkin-Elmer LS-55 fluorescence spectrophotometer. Thermogravimetric analysis (TGA) was carried out from room temperature to 800°C using a TGA/SDTA851e under N_2 at a heating rate of $10°C\,min^{-1}$.

2.2. *Synthesis of $[Co(6\text{-}BA\text{-}H_2)_2(H_2O)_4]\cdot(R)_2\cdot 4.5H_2O$ (1)*

Compound **1** was synthesized by the reaction of $CoCl_2\cdot 6H_2O$ 0.27 g (1.2 mmol), 6-BA 0.045 g (0.2 mmol), and 5-sulfosalicylic acid 0.10 g (0.4 mmol) in ethanol, dilute NaOH solution, and deionized water (3 : 0.15 : 4, v/v). The mixture was stirred for 40 min and placed in a 15 mL test tube for 15 days at room temperature. The initial and final values of pH are about 6.0 and 3.0. Light pink crystals of **1** were collected by vacuum filtration and dried in air (yield 23%). Anal. Calcd for $CoC_{38}H_{49}N_{10}O_{20.5}S_2$ (%): C, 41.57; H, 4.47; N, 12.76. Found: C, 41.53; H, 4.38; N, 12.69. IR data (cm^{-1}): 3398(m), 3222(m), 3033(w), 2929(w), 1668(s), 1623(w), 1585(m), 1475(w), 1427(s), 1355(m), 1255(m), 1180(s), 1124(m), 1079(w), 1035(s), 989(w), 869(w), 836(w), 780(w), 721(w), 673(m), 593(m), 451(w). The experimental data for **1** are in agreement with the simulated powder X-ray patterns based on single-crystal X-ray analysis, indicating the phase purity of the as-synthesized samples (figures S1a (IR) and S2a (XRD), see "Supplementary material").

2.3. *Synthesis of $[Co(6\text{-}BA\text{-}H)_2(H_2O)Cl_3]Cl\cdot H_2O$ (2)*

Compound **2** was synthesized by the reaction of $CoCl_2\cdot 6H_2O$ 0.045 g (0.2 mmol), 6-BA 0.045 g (0.2 mmol), and 0.04 mL HCl ($6\,molL^{-1}$) in ethanol and deionized water (4 : 1, v/v). The mixture was stirred for 40 min and placed in a 15 mL test tube for 15 days at room temperature. Initial and final values of pH are 2.0 and 1.6, respectively.

Dark pink rod-like crystals of **2** were collected by vacuum filtration and dried in air (yield 11%). Anal. Calcd for $CoC_{24}H_{28}N_{10}O_2C_{l4}$ (%): C, 41.78; H, 4.06; N, 20.31. Found: C, 41.70; H, 3.98; N, 20.19. IR data (cm^{-1}): 3427(m), 3384(m), 3191(m), 3143(w), 3022(m), 2879(w), 1652(s), 1621(m), 1585(m), 1473(w), 1448(m), 1396(m), 1340(m), 1278(w), 1209(m), 1162(w), 1118(m), 1081(w), 1026(w), 978(w), 885(w), 806(w), 755(m), 700(w), 663(w), 607(m), 539(m), 478(m). The experimental data for **2** are in agreement with the simulated powder X-ray patterns based on single-crystal X-ray analysis, indicating the phase purity of the as-synthesized samples (figures S1b (IR) and S2b (XRD), see "Supplementary material").

2.4. *X-ray crystallography*

Single crystals of **1** and **2** were mounted on a Bruker SMART APEX II diffractometer equipped with graphite-monochromated Mo-Kα radiation (0.71073 Å). Intensity data were collected at 296 ± 2 K and processed on a *PC* with the SAINT Plus software package. The structure was solved by direct methods and refined by full-matrix least-squares fitting on F^2 by *SHELXTL-97* [14]. All non-hydrogen atoms of **1** and **2** were refined with anisotropic thermal parameters. The positions of hydrogen atoms were either located by difference Fourier maps or calculated geometrically and their contributions in structural factor calculations included. For more details see the CIF files and Supplementary material. Crystallographic data of the crystal and refinements are summarized in table 1, selected bond lengths (Å) and angles (°) in table 2, and hydrogen bond lengths (Å) and angles (°) in table 3.

Table 1. Crystal data and structure refinements for **1** and **2**.

Compounds	**1**	**2**
Empirical formula	$C_{76}H_{98}Co_2N_{20}O_{41}S_4$	$C_{24}H_{28}C_{l4}CoN_{10}O_2$
Formula weight	2193.84	689.29
Temperature (K)	296(2)	296(2)
Wavelength (Å)	0.71073	0.71073
Crystal system	Monoclinic	Monoclinic
Space group	$P2/c$	$P2_1$
Unit cell dimensions (Å, °)		
a	7.707(3)	7.022(4)
b	8.679(3)	28.449(1)
c	35.234(1)	7.767(4)
β	102.616(8)	109.623(7)
Volume (Å^3), Z	2299.9(1), 1	1353.3(3), 2
Calculated density ($Mg\,m^{-3}$)	1.584	1.566
Absorption coefficient (mm^{-1})	0.557	0.996
$F(000)$	1140	706
θ range for data collection (°)	1.18–25.99	1.43–25.00
Reflections collected/unique	16,632/4487 [$R(\text{int}) = 0.0794$]	7365/4951 [$R(\text{int}) = 0.0415$]
Completeness to $\theta = 25.00$ (%)	98.8	99.8
Data/restraints/parameters	4487/0/327	4951/1/365
Goodness-of-fit on F^2	1.029	0.986
Final R indices [$I > 2\sigma(I)$]	$R_1 = 0.061$, $wR_2 = 0.1568$	$R_1 = 0.066$, $wR_2 = 0.1539$
R indices (all data)	$R_1 = 0.1087$, $wR_2 = 0.1819$	$R_1 = 0.0984$, $wR_2 = 0.1836$
Largest difference peak and hole ($e\text{Å}^{-3}$)	0.864 and −0.694	0.636 and −0.554

Table 2. Selected bond lengths (Å) and angles (°) for **1** and **2**.

1			
Co(1)–O(9)	2.045(4)	Co(1)–N(1)$^{\#1}$	2.166(4)
Co(1)–O(8)	2.058(4)	O(1)–S(1)	1.452(3)
Co(1)–O(7)$^{\#1}$	2.116(3)	O(2)–S(1)	1.446(3)
Co(1)–O(7)	2.116(3)	O(3)–S(1)	1.450(3)
Co(1)–N(1)	2.166(4)		
O(9)–Co(1)–O(8)	180.00(2)	O(7)$^{\#1}$–Co(1)–N(1)	92.42(1)
O(9)–Co(1)–O(7)$^{\#1}$	91.98(8)	O(7)–Co(1)–N(1)	87.67(1)
O(8)–Co(1)–O(7)$^{\#1}$	88.02(8)	O(9)–Co(1)–N(1)$^{\#1}$	88.75(9)
O(9)–Co(1)–O(7)	91.98(9)	O(8)–Co(1)–N(1)$^{\#1}$	91.25(9)
O(8)–Co(1)–O(7)	88.02(8)	O(7)$^{\#1}$–Co(1)–N(1)$^{\#1}$	87.67(1)
O(7)$^{\#1}$–Co(1)–O(7)	176.04(2)	O(7)–Co(1)–N(1)$^{\#1}$	92.41(1)
O(9)–Co(1)–N(1)	88.75(9)	N(1)–Co(1)–N(1)$^{\#1}$	177.49(2)
O(8)–Co(1)–N(1)	91.25(9)		
2			
Co(1)–O(1)	2.095(6)	Co(1)–Cl(4)	2.458(3)
Co(1)–N(6)	2.148(7)	Co(1)–Cl(3)	2.465(2)
Co(1)–N(1)	2.161(7)	Co(1)–Cl(2)	2.476(3)
O(1)–Co(1)–N(6)	89.8(3)	N(1)–Co(1)–Cl(3)	90.3(2)
O(1)–Co(1)–N(1)	91.2(3)	Cl(4)–Co(1)–Cl(3)	96.53(1)
N(6)–Co(1)–N(1)	178.9(3)	O(1)–Co(1)–Cl(2)	86.95(2)
O(1)–Co(1)–Cl(4)	83.45(2)	N(6)–Co(1)–Cl(2)	89.0(2)
N(6)–Co(1)–Cl(4)	91.2(2)	N(1)–Co(1)–Cl(2)	91.5(2)
N(1)–Co(1)–Cl(4)	88.5(2)	Cl(4)–Co(1)–Cl(2)	170.40(1)
O(1)–Co(1)–Cl(3)	178.5(2)	Cl(3)–Co(1)–Cl(2)	93.07(1)
N(6)–Co(1)–Cl(3)	88.7(2)		

Symmetry transformations used to generate equivalent atoms: $^{\#1}$ $-x+2$, y, $-z+1/2$.

3. Results and discussion

3.1. *Crystal structural studies*

3.1.1. Structure of $[Co(6\text{-}BA\text{-}H_2)_2(H_2O)_6]\cdot(R)_2\cdot 2.5H_2O$ (1). The asymmetric unit of 1 (figure 1a, scheme 1) contains a crystallographically independent Co(II), a 6-BAH_2^{2+}, three aqua ligands as well a free R^{3-} anion and three lattice water molecules. Co(1) is six-coordinate with two nitrogen atoms (N(1)) from two 6-BAH_2^{2+} ligands and four water oxygen atoms (O(7), O(7A), O(8), O(9)) to form its octahedral coordination geometry. Co–O/N bond distances ranging from 2.045(4) to 2.166(4) Å, *cis*-angles of 87.67(1)° to 91.25(9)°, and *trans*-angles of 176.04(2)–180.00(2) are close to those of reported metal 6-BA derivatives [9]. The coordinating pattern of 6-BA in **1** is monodentate bridging, affording one nitrogen N(1) to bridge Co(II). The remaining nitrogen atoms (N(2), N(3), N(5)) are involved in the formation of hydrogen bonds, along with the free R^{3-} and free water molecules. On the basis of charge balance, both N(3) and N(4) are protonated (these hydrogen atoms located from the difference Fourier map and refined isotropically).

Compound **1** displays a mononuclear molecular unit $[Co(6\text{-}BAH_2)_2(H_2O)_4]^{6+}$; two R^{3-} anions lie on the boat built from $[Co(6\text{-}BAH_2)_2(H_2O)_4]^{6+}$ and are joined *via* hydrogen bond O(9)–H(9A)···O(1) (2.632(4) Å, 161.2°) to form a neutral boat-like secondary building unit (SBU) $[Co(6\text{-}BAH_2)_2(R)_2]$. The key to the extended 1-D fishbone-like supramolecular chain is links of boat-like SBUs along the *a*-axis through hydrogen-bond interactions O(12)–H(12A)···O(7) (3.005(1) Å, 178.8°) (figure 1b). Adjacent 1-D chains are connected with each other *via* π–π stacking

Table 3. Hydrogen bond lengths (Å) and angles (°) for **1** and **2**.

D–H···A	d(D–H)	d(H···A)	d(D···A)	∠(DHA)
1				
N(2)–H(2A)···O(4)$^{\#2}$	0.86	1.92	2.760(5)	166.3
N(3)–H(3)···O(11)$^{\#3}$	0.86	1.95	2.786(6)	163.0
N(5)–H(5A)···O(5)$^{\#2}$	0.86	1.94	2.744(5)	155.6
O(7)–H(7B)···O(4)$^{\#4}$	0.85	1.92	2.714(4)	154.2
O(7)–H(7A)···O(11)$^{\#5}$	0.89	2.12	2.885(6)	144.5
O(7)–H(7A)···N(3)$^{\#1}$	0.89	2.68	3.394(5)	138.8
O(8)–H(8A)···O(10)$^{\#6}$	0.85	1.91	2.741(4)	166.0
O(9)–H(9A)···O(1)$^{\#1}$	0.85	1.81	2.632(4)	161.2
O(10)–H(10A)···O(3)	0.85	2.29	2.818(5)	120.9
O(10)–H(10A)···O(4)$^{\#7}$	0.85	2.52	3.216(5)	139.9
O(10)–H(10B)···O(3)$^{\#5}$	0.85	2.13	2.926(5)	155.0
O(10)–H(10B)···S(1)$^{\#5}$	0.85	2.88	3.585(4)	141.8
O(11)–H(11A)···O(10)	0.85	2.04	2.880(5)	168.1
O(11)–H(11B)···O(2)	0.85	1.98	2.754(5)	150.0
O(12)–H(12A)···O(7)	0.85	2.15	3.005(1)	178.8
2				
O(3)–H(3B)···Cl(2)$^{\#8}$	0.85	2.46	3.299(1)	168.4
O(3)–H(3A)···Cl(4)	0.85	2.26	3.093(1)	168.0
O(1)–H(1A)···Cl(3)$^{\#3}$	0.85	2.59	3.312(7)	143.4
O(1)–H(1B)···O(3)$^{\#9}$	0.85	1.84	2.664(1)	162.4
N(10)–H(10A)···Cl(1)$^{\#10}$	0.86	2.43	3.283(8)	170.6
N(9)–H(9A)···Cl(4)	0.86	2.85	3.413(8)	124.7
N(9)–H(9A)···Cl(3)$^{\#3}$	0.86	2.50	3.214(8)	141.6
N(7)–H(7)···Cl(1)$^{\#10}$	0.86	2.28	3.095(7)	159.2
N(5)–H(5)···Cl(1)	0.86	2.57	3.408(8)	166.0
N(3)–H(3)···Cl(2)	0.86	2.36	3.103(8)	144.4
N(2)–H(2)···Cl(1)	0.86	2.24	3.074(7)	161.9
C(4)–H(4)···Cl(3)$^{\#9}$	0.93	2.57	3.396(1)	147.8
C(18)–H(18B)···Cl(1)$^{\#11}$	0.97	2.79	3.717(1)	159.5

Symmetry transformations used to generate equivalent atoms: $^{\#1}-x+2, y, -z+1/2$; $^{\#2}x-1, y+1, z$; $^{\#3}x+1, y, z$; $^{\#4}-x+2, y+1, -z+1/2$; $^{\#5}-x+1, y, -z+1/2$; $^{\#6}-x+1, y+1, -z+1/2$; $^{\#7}x-1, y, z$; $^{\#8}x+1, y, z+1$; $^{\#9}x, y, z-1$; $^{\#10}-x, y-1/2, -z+1$; $^{\#11}-x+1, y-1/2, -z+1$.

interactions from between rings C(14)–C(15)–C(16)–C(17)–C(18)–C(19) (code: $-x$, $1-y$, $-z$, centroid distance 3.7042 Å, perpendicular distance 3.582 Å, dihedral angle 0.00°, slippage 0.943 Å) to develop into a 2-D supramolecular layer structure in the *ac* plane (figure 1b). The remaining hydrogen bonds extend the 2-D layer into a 3-D supramolecular framework (figure 1c). Hydrogen bonds formed by the other free water molecules (O···O, N···O, O···S) further consolidate the stability of **1**. The O···O (2.6–2.8 Å) and N···O (2.7–2.8 Å) hydrogen bonds are slightly stronger than those of reported compounds [8–13].

3.1.2. Structure of $[Co(6\text{-}BA\text{-}H)_2(H_2O)Cl_3]Cl \cdot H_2O$ (2). The asymmetric unit of 2 (figure 2a) contains a crystallographically independent Co(II), two 6-BAH$^+$ cations, a coordinated water, three coordinated Cl$^-$, a free Cl$^-$, and a lattice water molecule. Co(1) is octahedrally coordinated by two nitrogen atoms (N(1), N(6)) from two 6-BAH$^+$ ligands, one water molecule (O(1)) and three Cl$^-$ to form a distorted chair-like molecular geometry. Co–O/N bond distances range from 2.095(6) to 2.161(7) Å, Co–Cl bond distances are 2.458(3) Å, 2.465(2) Å, and 2.476(3) Å. The cis-angles of O/N/Cl–Co–N/Cl range from 83.45(2)° to 96.53(1)° and trans-angles are 170.40(1)°–178.9(1)°. These bond lengths and angles are close to those of reported metal 6-BA compounds [9, 13]. The coordination pattern of 6-BA in 2 is similar to that of 1. The difference is that only nitrogen (N(3)/N(9)) of each 6-BA is protonated for charge balance. The remaining nitrogen atoms are involved in the formation of hydrogen bonds, along with the Cl$^-$ and the coordinated water.

Compound **2** exhibits a mononuclear molecular structure $[\mathrm{Co}(6\text{-BAH})_2(\mathrm{H_2O})\mathrm{Cl_3}]^+$ with a positive charge. Rings are labeled as follows: C(19)–C(20)–C(21)–C(22)–C(23)–C(24) marked R1, N(3)–C(3)–C(2)–C(5)–N(4)–C(4) marked R2, N(1)–C(1)–N(2)–C(2)–C(3) marked R3, C(7)–C(8)–C(9)–C(10)–C(11)–C(12) marked R4, N(8)–C(16)–N(9)–C(15)–C(14)–C(17) marked R5, N(6)–C(13)–N(7)–C(14)–C(15) marked R6. Mononuclear units $\left[\mathrm{Co}(6\text{-BAH})_2(\mathrm{H_2O})\mathrm{Cl_3}\right]_n^+$ are interconnected to set up 1-D zigzag supramolecular chains along the *b*-axis

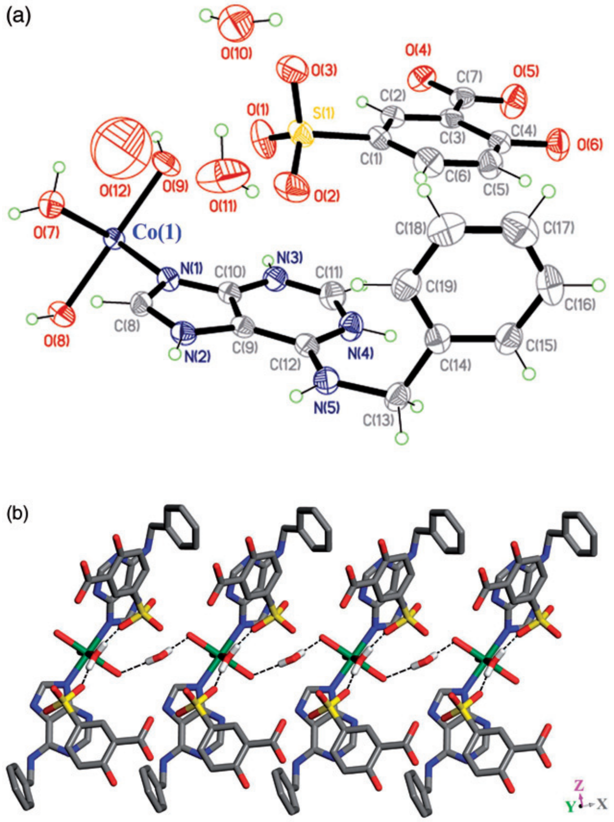

Figure 1. (a) ORTEP view of **1** showing the atom-labeling scheme (40% thermal ellipsoids). (b) 1-D supramolecular fishbone-like chain of **1** *via* H-bonds along the *a*-axis. Hydrogen bonds are drawn as dotted lines. (c) 2-D supramolecular framework formed by H-bonds and π–π stacking interactions in the *ac* plane. (d) 3-D supramolecular framework *via* H-bonds and π–π stacking interactions along the *x*-axis. Hydrogen bonds and π–π stacking are drawn as dotted lines. For clarity all hydrogen atoms are omitted except those of lattice water molecules.

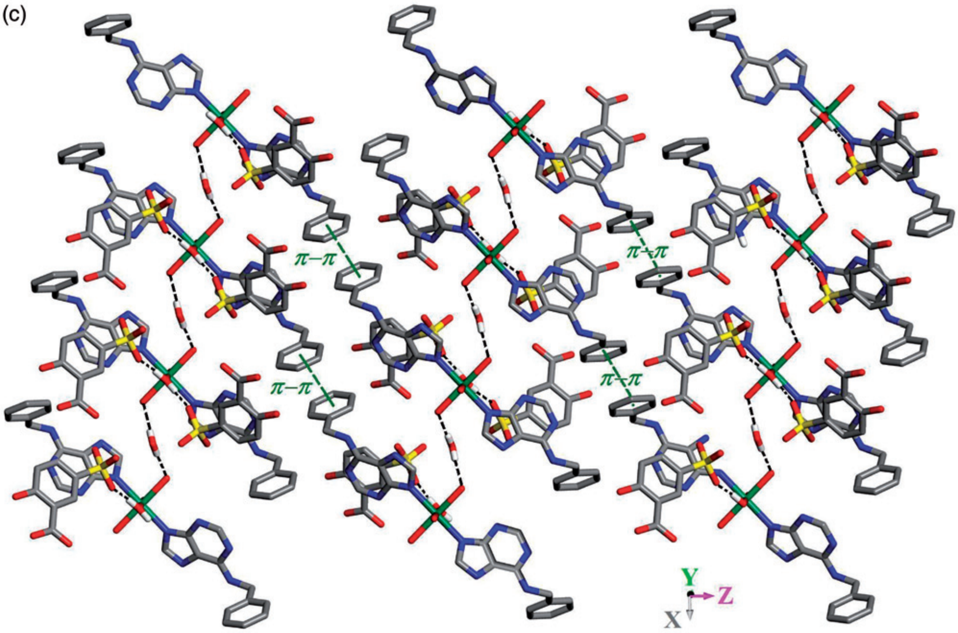

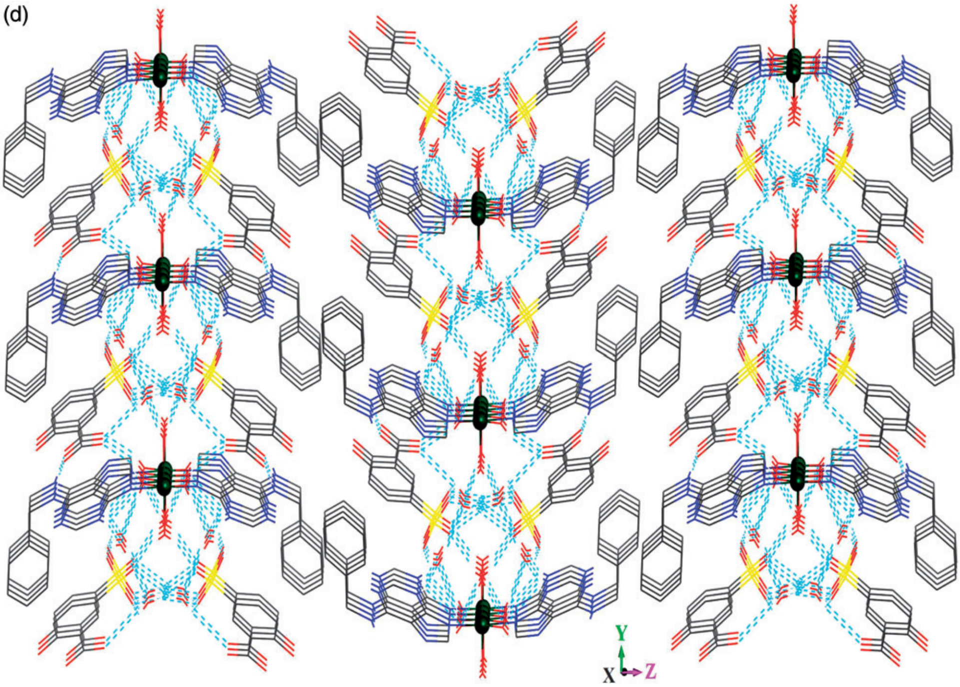

Figure 1. Continued.

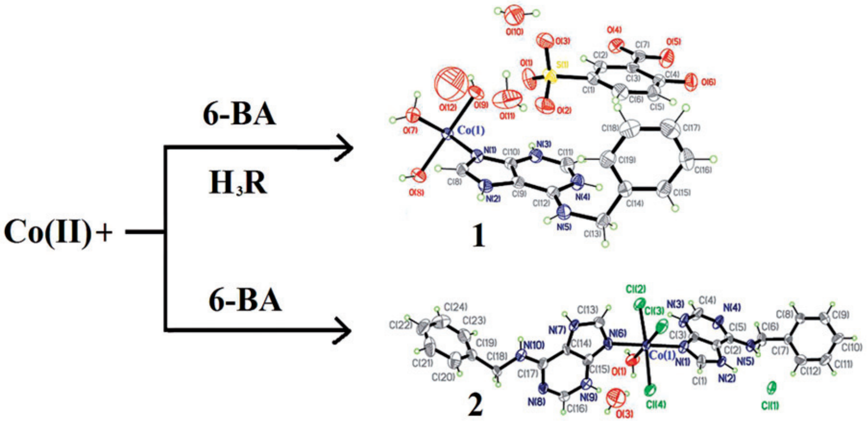

Scheme 1. Routes and molecular structures of **1** and **2**.

(figure 2b) through three kinds of hydrogen bonds, C(18)–H(18B)$\cdots$Cl(1) (3.717(1) Å, 159.5°), N(2)–H(2)$\cdots$Cl(1) (3.074(7) Å, 161.9°) and N(5)–H(5)$\cdots$Cl(1) (3.408(8) Å, 166.0°), and π-stacking interactions between R1 and R2 rings (code: $1-x$, $-1/2+y$, $1-z$, centroid distance 3.7713 Å, dihedral angle 6.54°, perpendicular distance 3.451/3.597 Å, slippage 1.521/1.133 Å), and between R1 and R3 rings (code: $2-x$, $-1/2+y$, $1-z$, centroid distance 3.9268 Å, dihedral angle 5.43°, perpendicular distance 3.500/3.400 Å, slippage 1.78/1.96 Å). In the *ab* plane, four kinds of hydrogen bonds and π-stacking interactions further extend the 1-D zigzag supramolecular chain into a 2-D supramolecular layer structure (figure 2c), with corresponding hydrogen bonds O(1)–H(1A)$\cdots$Cl(3) (3.312(7) Å, 143.4°), N(9)–H(9A)$\cdots$Cl(3) (3.214(8) Å, 141.6°), N(7)–H(7)$\cdots$Cl(1) (3.095(7) Å, 159.2°) and N(10)–H(10A)$\cdots$Cl(1) (3.283(8) Å, 170.6°), and π-stacking modes between R1 and R3 rings (code: $1-x$, $-1/2+y$, $1-z$, centroid distance 3.8206 Å, dihedral angle 5.43°, perpendicular distance 3.485/3.486 Å, slippage 1.566/1.563 Å), and between R1 and R2 rings (code: $2-x$, $-1/2+y$, $1-z$, centroid distance 4.1367 Å, dihedral angle 6.54°, perpendicular distance 3.541 Å, slippage 2.14 Å). A 3-D supramolecular framework (figure 2d) is formed *via* an important hydrogen bond, C(4)–H(4)$\cdots$Cl(3) (3.396(10) Å, 147.8°), and π-stacking interactions between R4 and R6 rings (code: $2-x$, $1/2+y$, $2-z$, centroid distance 3.8310 Å, dihedral angle 0.04°, perpendicular distance 3.656 Å, slippage 1.144 Å), and between R4 and R5 rings (code: $2-x$, $1/2+y$, $2-z$, centroid distance 3.9094 Å, dihedral angle 0.19°, perpendicular distance 3.651/3.656 Å, slippage 1.40/1.39 Å). Various hydrogen bonds (C$\cdots$Cl, N$\cdots$Cl, O$\cdots$Cl, O$\cdots$O) and π-stacking interactions exist in **2**. C$\cdots$Cl ($3.3\sim3.7$ Å), O$\cdots$O ($2.6\sim2.7$ Å), O$\cdots$Cl ($3.0\sim3.3$ Å), and N$\cdots$Cl ($3.0\sim3.4$ Å) hydrogen bonds are slightly stronger than those of related compounds [8–13].

3.2. *Thermal analyses*

TG-DTA analyses (figure 3) examine the stabilities of both the compounds under N_2. The TGA curve of $[Co(6\text{-}BA\text{-}H_2)_2(H_2O)_4]\cdot(R)_2\cdot4.5H_2O$ is three weight loss steps. A small endothermic peak at 125°C from 85°C to 150°C is attributed to release of lattice water molecules, aqua ligands and –OH group. The weight loss of 15.4% is in good agreement with the calculated value (15.5%). The second step of 41.1% from 235°C and 350°C corresponds to pyrolysis of 6-BAH$_2$ (Calcd 41.4%). The last step of 37.9% starts at 350°C, owing chiefly to continued collapse of H$_3$R, and completes at 620°C (Calcd 37.6%). There are three small exothermic peaks at 324°C, 490°C, and 545°C in the DTA curve. The main residue is Co, based on XRD powder studies and the value of 5.6% is close to the calculated (5.3%). The thermolysis of **2** contains three main

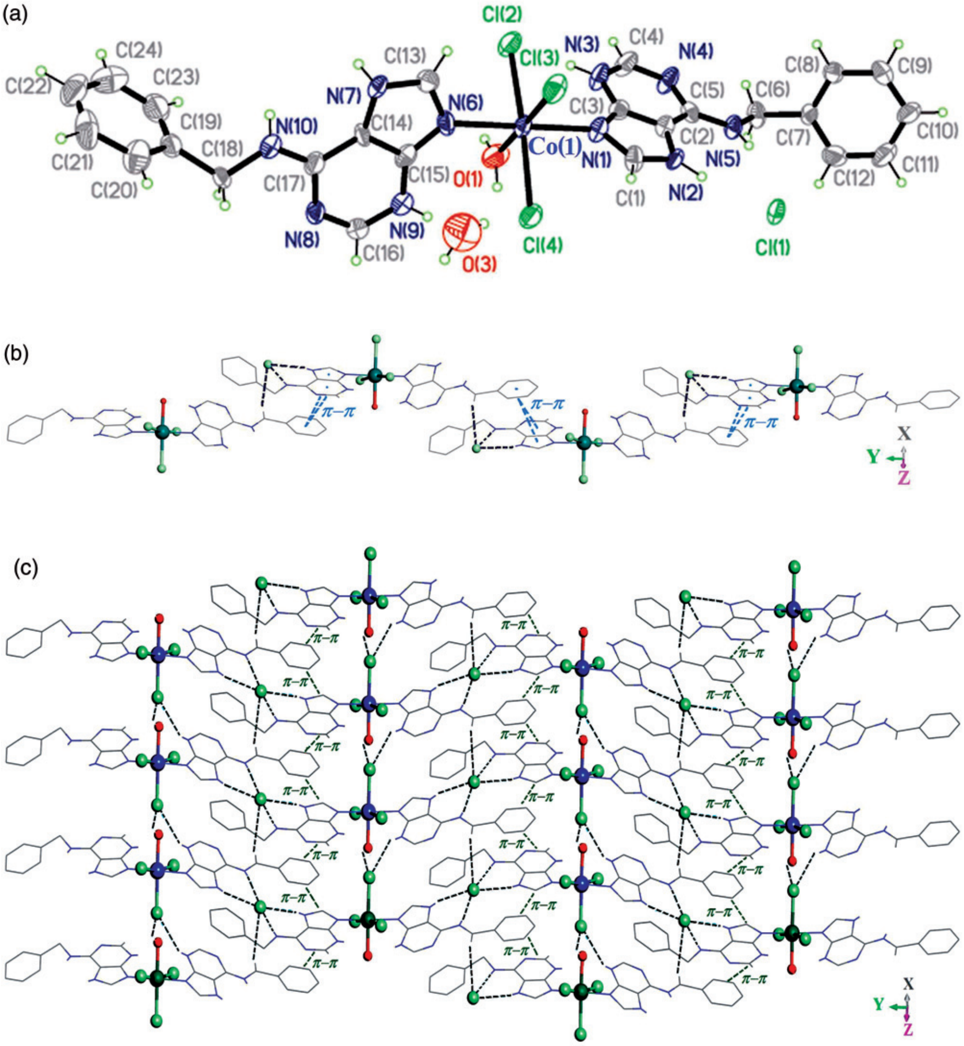

Figure 2. (a) ORTEP view of **2** showing the atom-labeling scheme (40% thermal ellipsoids). (b) 1-D supramolecular zigzag chain of **2** *via* H-bonds and π–π stacking interactions along the *b*-axis. (c) 2-D supramolecular framework in the *ab* plane *via* H-bonds and π–π stacking interactions. (d) 3-D supramolecular network *via* H-bonds and π–π stacking interactions along the *x*-axis. Hydrogen bonds and π–π stacking are drawn as dotted lines. The free H$_2$O molecules and all hydrogen atoms are omitted for clarity except those of C(18) and nitrogen.

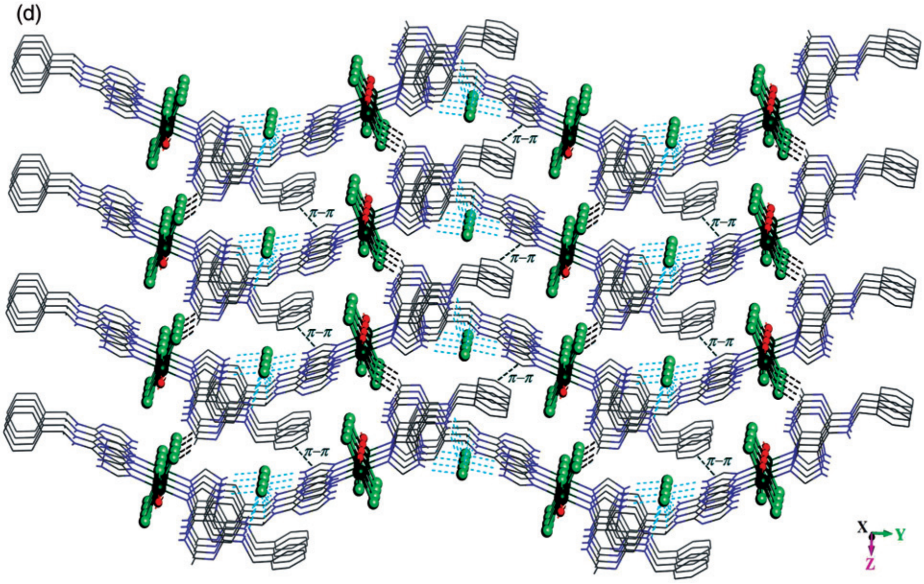

Figure 2. Continued.

steps (figure 3), starting at 90°C. The first weight loss from 90°C to 160°C with an endothermic peak at 148°C of 5.4% is due to the release of two H_2O molecules (Calcd 5.2%). The second and third steps of 86.2% is continuous decomposition stages from 254°C, corresponding to the pyrolysis of 6-BAH_2 and liberation of Cl^-. The last two steps complete at 650°C being accompanied by three small exothermic peaks at 322°C, 369°C, and 572°C, indicating collapse of the organic framework (Calcd 85.8%). The main residue (8.8%) agrees with Co based on XRD powder studies (Calcd 8.5%).

3.3. *UV-Vis absorption analyses*

The UV-Vis absorption spectrum of **1** in ethanol is shown in figure 4. Bands centered at 207.2 nm and 267.7 nm for **1** and 268.2 nm for **2** reveal that the absorptions are mainly from 6-BAP (207.8 nm, 267.5 nm) [15], slightly red-shifted from protonation of 6-BAP.

3.4. *Fluorescence studies*

The fluorescence of both compounds and 6-BA/H_3R are shown in figure 5. Free 6-BA emits three strong fluorescence peaks centered at 318.9 nm, 382.8 nm, and 434.0 nm ($\lambda_{ex} = 235$ nm), whereas the H_3R ligand shows shoulders centered at 387.4 nm and 438.0 nm ($\lambda_{ex} = 270$ nm). Upon 6-BA-complexation with two different ligands H_3R/Cl^- on Co(II), **1** ($\lambda_{ex} = 268$ nm) displays two stronger fluorescent emissions centered at 326.8 nm and 356.9 nm, but **2** ($\lambda_{ex} = 233$ nm) exhibits a weaker peak at 342.8 nm. The emission spectra of **1** and **2** are neither metal-to-ligand charge transfer (MLCT) nor ligand-to-metal charge transfer (LMCT), but rather are intraligand π^*–π emissions.

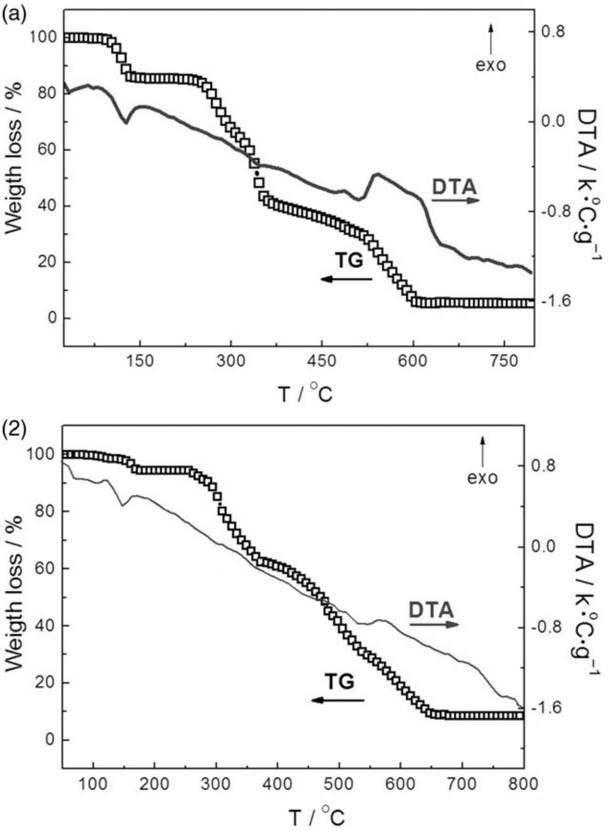

Figure 3. The TG-DTA curves of **1** and **2**.

Emission bands of **1** and **2** are blue-shifted which suggests they may be candidates as acceptors in the Co(II)-6-BA system. The fluorescent intensity of **1** is more than eight times that of **2**, largely due to cooperativity of 6-BA and H_3R. 5-Sulfosalicylic acid (H_3R) for **1** not only effectively increases the rigidity but also suppresses the loss of energy. The fluorescent spectrum of **2** however shows a significant decrease in intensity compared with that of the 6-BA ligand, derived from coordination of the 6-BA with Co(II).

4. Conclusions

We have obtained two new mononuclear Co(II)-6-BA supramolecular compounds, $[Co(6\text{-}BA\text{-}H_2)_2(H_2O)_4]\cdot(R)_2\cdot4.5H_2O$ (**1**) and $[Co(6\text{-}BA\text{-}H)_2(H_2O)Cl_3]Cl\cdot H_2O$ (**2**). Compound **1** possess a 3-D supramolecular structure with mononuclear cation $[Co(6\text{-}BA\text{-}H_2)_2(H_2O)_4]^{6+}$ in which the Co(II) is six-coordinate and two nitrogen atoms (N(3), N(4)) are protonated. Compound **2** also exhibits a 3-D supramolecular framework with mononuclear $[Co(6\text{-}BA\text{-}H)_2(H_2O)Cl_3]^{+}$ in which only N(9) is

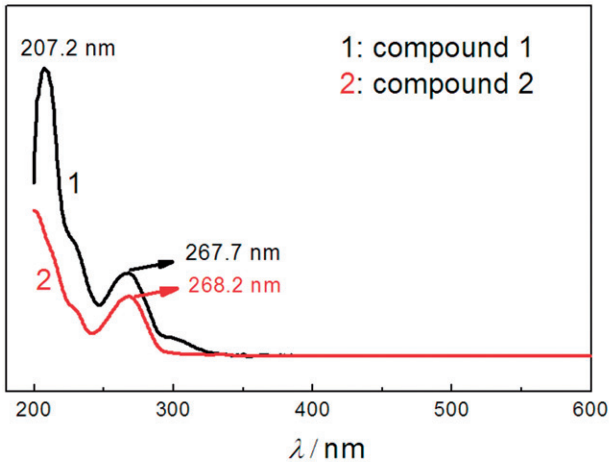

Figure 4. UV-Vis absorption spectra of **1** and **2**.

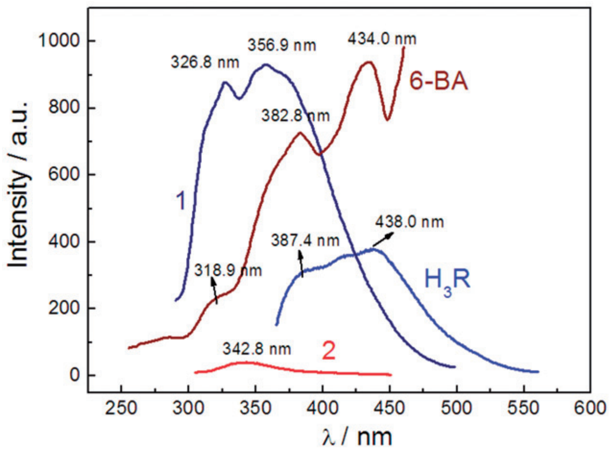

Figure 5. Solid-state emission spectra of **1** and **2** and ligands.

protonated within 6-BA. Meanwhile, luminescent properties at room temperature show fluorescent emission bands at 326.8 nm and 356.9 nm for **1** ($\lambda_{ex} = 268$ nm), and 342.8 nm for **2** at the excitation of 233 nm, caused by intraligand π–π^* transition.

Supplementary material

CCDC Nos 748912 (**1**) and 836353 (**2**) contain the supplementary crystallographic data. These data can be obtained *via* the Cambridge Crystallographic Data Centre (deposit@ccdc.cam.ac.uk; http://www.ccdc.cam.ac.uk/deposit).

References

[1] G.K.H. Shimizu, R. Vaidhyanathan, J.M. Taylor. *Chem. Soc. Rev.*, **38**, 1430 (2009).

[2] V. Videnova-Adrabinska. *Coord. Chem. Rev.*, **251**, 1987 (2007).

[3] P.J. Davies. *Plant Hormones: Biosynthesis, Signal Transduction, Action!*, p. 241, Kluwer Academic Publishers, Dordrecht, Boston, London (2004).

[4] R.M. Goldsteyn. *Cancer Lett.*, **217**, 129 (2005).

[5] F.I. Raynaud, S.R. Whittaker, P.M. Fisher, S. McClue, M.I. Walton, S.E. Barrie, M.D. Garrett, P. Rogers, S.J. Clarke, L.R. Kelland, M. Valenti, L. Brunton, S. Eccles, D.P. Lane, P. Workman. *Clin. Cancer Res.*, **11**, 4875 (2005).

[6] Z. Trávnácěk, L. Szücvá, I. Popa. *Inorg. J. Biochem.*, **101**, 477 (2007).

[7] V. Pattabhi. *Curr. Sci.*, **59**, 1233 (1990).

[8] Z. Trávníček, M. Matiková-Maarová, R. Novotná, J. Vančo, K. Štěpánková, P. Suchý. *J. Inorg. Biochem.*, **105**, 937 (2011).

[9] A. Klanicová, Z. Trávníček, J. Vančo, I. Popa, Z. Šindelář. *Polyhedron*, **29**, 2582 (2010).

[10] F. Ohashi, S. Ueda, T. Taguri, S. Kawachi, H. Abe. *Appl. Clay Sci.*, **46**, 296 (2009).

[11] J. Ribas, M. Monfort, R.C.X. Solans. *Inorg. Chim. Acta*, **157**, 57 (1989).

[12] T.P. Balasubramanian, P.T. Muthiah, Ananthasaravanan, S.K. Mazumdar. *J. Inorg. Biochem.*, **63**, 175 (1996).

[13] N. Stanley, P.T. Muthiah, P. Luger, M. Weber, S.J. Geib. *Inorg. Chem. Commun.*, **8**, 1056 (2005).

[14] G.M. Sheldrick. *GM SHELXL-97*, University of Göttingen, Germany (1997).

[15] M. Xia, K.-R. Ma, Y.-L. Zhu. *J. Chem. Crystallogr.*, **40**, 634 (2010).